J. Phys.: Condens. Matter **10** (1998) 7445–7451. Printed in the UK PII: S0953-8984(98)94464-2

Evidence for a square vortex lattice in Sr_2RuO_4 from muon-spin-rotation measurements

C M Aegerter†, S H Lloyd‡, C Ager§, S L Lee§, S Romer†, H Keller† and E M Forgan‡

† Physik-Institut der Universität Zürich, CH-8057 Zürich, Switzerland
‡ School of Physics and Space Research, University of Birmingham, Birmingham B15 2TT, UK
§ School of Physics and Astronomy, University of St Andrews, St Andrews, Fife KY16 9SS, UK

Received 21 May 1998, in final form 23 June 1998

Abstract. A muon-spin-rotation study of the flux-line lattice in Sr_2RuO_4 is presented. For the field parallel to the crystallographic c-direction, the observed field distribution strongly indicates a square symmetry of the vortex lattice. We determine the value of the coherence length from the upper critical field and the Ginzburg–Landau parameter which is found to be $\kappa = 1.2(1)$ from the field distribution. This gives a value for the penetration depth of $\lambda = 185(15)$ nm. The temperature dependence of the penetration depth is measured.

The recent discovery of superconductivity in the perovskite compound Sr_2RuO_4 (SRO) has resulted in much increased experimental as well as theoretical research activity on this system [1]. Like the high-temperature superconductors (HTS), SRO is a layered compound. In fact, SRO is isostructural with the HTS $La_{2-x}Ba_xCuO_4$, but is the only known layered perovskite superconductor which does not contain copper. The striking difference in T_c between SRO ($T_c \sim 1$ K) and the HTS ($T_c \sim 100$ K) provides a challenge to theories which aim to explain superconductivity in these systems reflecting the different normal-state properties.

The related compound $SrRuO_3$ is ferromagnetic with a Curie temperature of ∼160 K. This has led to the proposal of p-wave superconductivity in SRO [2, 3], as the very strong correlations are assumed to exist down to the superconducting transition, favouring p-wave symmetry of the Cooper pairs. It has been argued that, as in the case of $SrRuO_3$, strong Hund's rule coupling would lead to preferential formation of spin-triplet pairing of the Ru moments [2, 3]. The superconducting transition T_c is much lower than the onset of well developed Fermi liquid behaviour observed in resistivity data [4], and the coupling is thought to be weak [2]. In the presence of nodes, weak-coupling p-wave superconductivity would be unstable, with the result that a nodeless p-wave gap is predicted [2]. Thus measurements of the temperature dependence of the penetration depth would not reveal any difference from conventional s-wave pairing, showing a saturation of $\lambda^{-2}(T)$ at low temperatures. In view of the above arguments, SRO is thought to be an analogue of the Balian–Werthamer state of superfluid ^{3}He [5], but with a lattice potential and hence of interest in its own right.

In order to investigate the effects of possible p-wave superconductivity, we may still study the temperature dependence of λ. Although we may not be able to distinguish between

0953-8984/98/337445+07$19.50

conventional s-wave pairing and the proposed nodeless p-wave pairing, a linear temperature dependence of λ at low temperatures indicates the existence of nodes in the gap. In the HTS such findings are usually connected with the proposed d-wave pairing in these systems. If there are nodes in the gap for SRO, this may indicate the presence of non-unitary states [6], or the occurrence of d-wave superconductivity. Muon-spin rotation (μSR) presents a very effective tool for measuring the penetration depth in a type-II superconductor. Together with neutron scattering and NMR, it is one of the very few *microscopic* methods investigating the *bulk* of the material, as the muons penetrate fractions of a millimetre into the sample.

The sample consisted of a mosaic of several Sr_2RuO_4 single crystals of typical size $4 \times 3 \times 0.2$ mm^3. The mosaic covered an area of approximately 1 cm^2. The crystals that made up the mosaic were also characterized by x-ray diffraction. This revealed that the samples had a mosaic spread of approximately 2°, and thus were not of perfect quality. This may also be associated with a certain amount of non-superconducting inclusions in the samples, as we shall discuss below. The experiment was carried out at the LTF instrument on beam line πM3 at the Paul Scherrer Institute (PSI), Villigen, Switzerland, with the field applied parallel to the crystallographic *c*-direction.

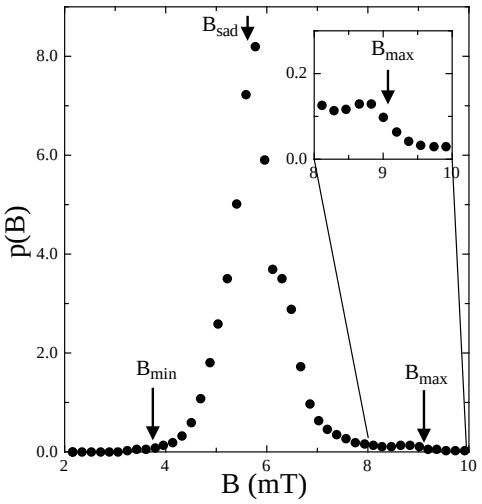

Figure 1. The field probability distribution measured in an applied field of 6 mT, with a background subtracted (see the text). The characteristic fields B_{min}, B_{sad} and B_{max} are clearly visible. Their relative positions are highly consistent with the expectations for a square lattice (see the text). We may then determine, together with the value of B_{c_2}, the value of the penetration depth λ. The inset shows a magnification around the maximum field B_{max}.

In a transverse-field μSR experiment, spin-polarized low-momentum muons are implanted in the sample at random, where they thermalize rapidly. The muon spins then precess in the local magnetic field at the site of rest. Due to parity violation, the decay positron is emitted preferentially in the direction of the muon spin, thus allowing the time evolution of the muon polarization to be measured. As the muons are implanted at random positions relative to the vortex lines, the real part of the Fourier transform of this time evolution corresponds to the probability distribution of local fields $p(B)$. In our analysis we used a maximum-entropy algorithm [7] to deduce the Fourier transform. This field probability distribution $p(B)$ is intimately related to the distribution of local fields $B(r)$ and for type-II superconductors in the mixed state can be calculated theoretically [8]. This field

distribution has some striking features, such as a tail extending to fields higher than the applied field, due to vortex core fields, and a cut-off corresponding to the maximum field in a flux line associated with the coherence length ξ, i.e. the core radius. Together with the mode of the field distribution (B_{sad}), which theoretically corresponds to saddle points in the local spatial distribution, this gives a measure of the two fundamental superconducting parameters λ and ξ. Usually, at least in the study of HTS materials, it is assumed that the London approximation, $B \ll B_{c_2}$, is valid. This however is not the case for SRO with B_{c_2} (in our sample) $\approx$ 13 mT. Thus to obtain correct values for λ and ξ, we have to use more sophisticated models. In the case of $B \lesssim B_{c_2}$, Sidorenko *et al* [8] have been able to analytically calculate the field distribution $p(B)$ from Abrikosov's solution of the Ginzburg–Landau equations. Thus we are able to obtain, together with the experimentally determined value of B_{c_2}, the penetration depth and the coherence length. In a different approach, we may use the scaling function recently derived by Yaouanc *et al* [14] to extend the London approximation for the full range of fields (see below).

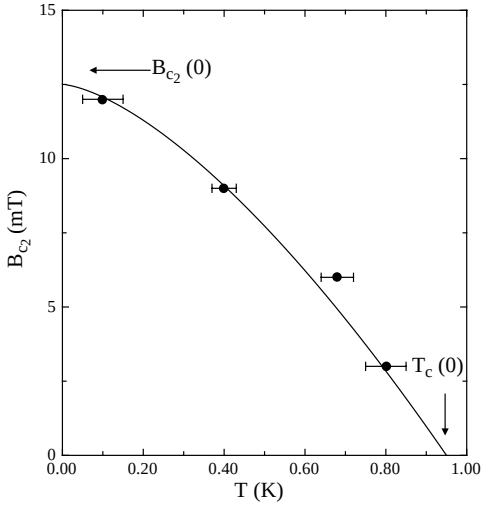

Figure 2. The temperature dependence of the upper critical field B_{c_2}, as determined from the broadening of the field distribution. This can be seen, e.g., in figure 3, where the temperature dependence of the μSR linewidth is shown for an applied field of 6 mT. The measurements follow the general form $B_{c_2}(T) = B_{c_2}(0)(1 - (T/T_c)^{1.5})$, as indicated by the solid line, with values of $T_c = 0.95$ K and $B_{c_2}(0) = 13$ mT, representing a measure of the coherence length ξ (see the text).

A typical field probability distribution from the mixed state in the sample is shown in figure 1. This was taken at an applied field of 6 mT and a temperature of 50 mK. The raw field distribution showed a background from muons precessing in the applied field. The sample was backed by an Fe_2O_3 plate, to rapidly depolarize, outside the observable time window, any muons not hitting the sample. Without a sample we do not detect any signal; thus such a background has to arise from non-superconducting inclusions in the crystals. For the field distribution in figure 1, a Gaussian distribution of a width of 0.22 mT (corresponding to the nuclear and instrumental broadening as measured in the normal state) and centred at the applied field was subtracted. The area of the Gaussian made up 20% of the lineshape. This subtraction allowed us to properly identify the characteristic fields B_{min}, B_{sad} and B_{max} that we use in our analysis. It has to be noted however that the minimum

and maximum fields are unchanged by the subtraction of the background, as they are far removed from the applied field.

In the Abrikosov approximation, all of the characteristic fields depend on

$$B_{c_2}/(1+\beta(2\kappa^2-1))$$

where β is a factor of order unity depending on the symmetry of the vortex lattice. Thus for obtaining an estimate of the Ginzburg–Landau parameter κ, the upper critical field B_{c_2} has to be known. In the μSR experiments, we determined the temperature dependence of B_{c_2} from the onset of the broadening of the field distribution, as a function of temperature at fixed B. Thus measuring T_c as a function of the applied field allows us to estimate the low $B_{c_2}(0)$ of SRO to good accuracy. In figure 2, we show the field dependence of T_c, resulting in an estimate of $T_c(0) = 0.95$ K and $B_{c_2}(0) = 13$ mT. These values are somewhat lower than usually quoted in the literature [4], with T_c-values extending up to 1.5 K and B_{c_2}-values of up to 70 mT. This may be due to the strong suppression of T_c by impurities [9] combined with the quality of the crystals used here. We may thus obtain the coherence length from $B_{c_2} = \Phi_0/2\pi\xi^2$ as $\xi = 155(15)$ nm. We may then also determine, together with the information obtained from the field distribution, the penetration depth λ and thus also the Ginzburg–Landau parameter κ.

It should be noted, however, that in the region of the measurements at a considerable fraction of B_{c_2}, the nature of the pairing might become important. This would affect the measurements mainly as regards changes of the lattice *structure*. Although the Abrikosov solution assumes an isotropic s-wave core, in contrast to the theoretical expectation that the pairing symmetry is of p-wave type in SRO, the field distribution is mainly affected by the structure of the vortex lattice as opposed to the exact field distribution of a single vortex line. We shall therefore consider the possibility that the overall structure of the vortex lattice may change to allow for changes induced by the vortex core, while calculating the lineshape corresponding to such a lattice structure from the Abrikosov solution. We may then compare the observed field distributions with predictions of different lattice morphologies in the Abrikosov limit. As in this case the characteristic fields B_{min}, B_{sad} and B_{max} are interdependent, the relative positions of these fields may be used to find a consistent description of the field distribution in terms of a vortex lattice morphology. From the calculations of Sidorenko *et al* [8] we find that the parameter

$$\gamma = \frac{B_{max} - B_{sad}}{B_{sad} - B_{min}} \tag{1}$$

differs strongly in the case of a hexagonal ($\gamma_\triangle = 8$) and square lattice ($\gamma_\square = 2.5$). In the experiment, we observe all three characteristic fields. In an applied field of 6 mT (see figure 1), the characteristic fields are $B_{min} = 3.8(2)$ mT, $B_{sad} = 5.5(1)$ mT and $B_{max} = 9.0(2)$ mT. This results in the experimental value of $\gamma_{6\,\mathrm{mT}} = 2.3(2)$, in good agreement with the expectation for a square lattice. Similar values can be found from the field distribution in an applied field of 3 mT, where we obtain $\gamma_{3\,\mathrm{mT}} = 2.3(3)$, again in very good agreement with the values for a square lattice. In this respect, we would also like to note that μSR represents a local measurement. Therefore static disorder will only be measured over a unit cell of the vortex lattice and is averaged over all unit cells in the final picture. Hence any static disorder present in the vortex lattice can be estimated from the smearing of the cut-off fields B_{min} and B_{max} [11]. This smearing is of the order of the instrumental resolution ($\langle\Delta B^2\rangle^{1/2} = 0.27(3)$ mT) and thus the static disorder in the lattice must be small. We thus conclude that, possibly due to some non-local interactions or in-plane anisotropy, the vortex lattice in SRO is of a square morphology, in agreement with recent neutron small-angle scattering (SANS) results [10]. It has to be noted however, that the flux

lattice structure may change as a function of field in conventional s-wave superconductors [12]. These effects have already been observed in members of the borocarbide family RNi_2B_2C [13].

Therefore we may now extract the G–L parameter κ from the characteristic fields, using the numerical predictions given in reference [8]. For this, we use B_{max}, as it is the most accurately determined. Using

$$B_{max} - \langle B \rangle = \frac{B_{c_2} - \langle B \rangle}{1 + 1.18(2\kappa^2 - 1)} \tag{2}$$

we find $\kappa = 1.2(1)$, resulting in a value of the penetration depth of $\lambda_{ab} = 185(15)$ nm. The value of the penetration depth may also be determined from a general solution to the G–L equations [14]. This gives a scaling function capable of extending the London approximation to fields comparable to B_{c_2}. In the London approximation, B_{sad} for a square lattice is given by [8]

$$(B_{sad} - \langle B \rangle) = -\frac{1}{2}\frac{\Phi_0}{4\pi\lambda^2} \ln 2 f(B/B_{c_2}) \tag{3}$$

where $\Phi_0 = h/2e$ is the flux quantum, and $f(b)$ is the scaling function calculated in reference [14]. Evaluating this function at 6 mT, where $B_{sad} - \langle B \rangle = -0.5$ mT, results in $f(0.4) \simeq 0.22$. This gives a value for the penetration depth of $\lambda_{ab} = 200(20)$ nm, consistent with the result obtained in the Abrikosov limit.

These values for the penetration depth are similar to those found in cuprate HTS [15]. However, the coherence length tends to vary inversely with T_c [16], and we find that ξ for SRO is ~100 times longer than for cuprates. This gives rise to substantial differences in the vortex behaviour in the HTS and SRO. Whereas the short coherence lengths ($\xi_c \ll$ layer spacing) of the HTS may lead to quasi-two-dimensional vortex behaviour (e.g. in BSCCO), SRO behaves more like a three-dimensional superconductor in spite of its considerable anisotropy. Moreover, due to the low value of $\kappa \simeq 1.2$, we might expect to observe a crossover from type-II superconducting behaviour to that of a type-I superconductor [17]. This, however, would necessitate a temperature dependence of κ originating in different temperature dependences of ξ and λ. The temperature dependence of the coherence length can be inferred from figure 2, where the temperature dependence of $B_{c_2} \propto 1/\xi^2$ is given.

In order to measure the temperature dependence of λ, we measured the width of the field distribution

$$\langle \Delta B^2 \rangle^{1/2} \propto (1/\lambda^2) f(b)$$

at different temperatures. A closer inspection of the temperature dependence of λ can also give insights into the pairing symmetry of the superconducting wavefunction, although several other quantities may have similar influences on the muon signal. At such low values of κ and low temperatures, the effect of thermal fluctuations of the flux lattice is small and can be neglected. In order to obtain the temperature dependence of λ^{-2} from that of $\langle \Delta B^2 \rangle^{1/2}$, the temperature dependence of B_{c_2} has to be taken into account as well. This is done by dividing the second moment by the function $f(b)$ [14] (see also equation (3)). The result of this is shown in figure 3. In the plot, instrumental and nuclear broadening have been taken into account by subtracting the second moment in the normal state from that in the superconducting state. As can be seen in the figure, the temperature dependence of $1/\lambda^2(T)$ can be represented by a linear function over most of the temperature range. Comparing this with the temperature dependence of the coherence length, we find very similar behaviour, leading to a constant value of κ with temperature change and hence no crossover to a type-I superconductor. Concerning the symmetry of the wavefunction, a supposed p-wave

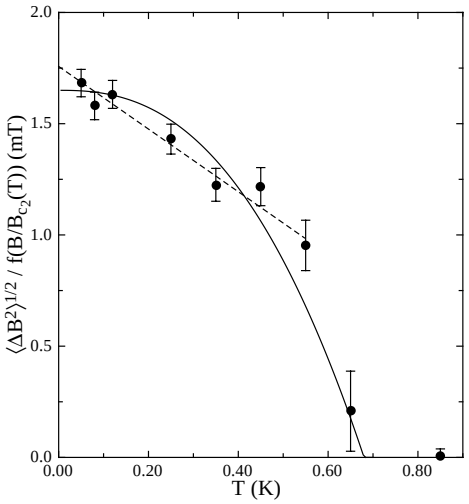

Figure 3. The temperature dependence of the μSR linewidth $\langle \Delta B^2 \rangle^{1/2}$ corrected for the temperature dependence of B_{c_2} for an applied field of 6 mT. The variance of the field distribution in the normal state has been subtracted. This presents a measure of the temperature dependence of the penetration depth $\lambda(T)$. The temperature dependence can be represented by a linear function at low temperatures (dashed line), but may however also be fitted with a BCS-like temperature dependence (solid line). A linear temperature dependence would indicate the presence of nodes, inconsistent with a simple constant-gap p-wave symmetry of the superconducting pairs (see the text).

state having no nodes should show saturation of $\lambda^{-2}(T)$ at low temperatures, similar to the expectations for an s-wave superconductor. The data presented in figure 3 are consistent with a linear temperature dependence at low temperatures similar to that found in the HTS [18]. This is usually taken to indicate the presence of nodes, which is inconsistent with the theoretical expectations [2]. The data are however also consistent with a power-law expression of the form

$$\lambda^{-2}(T) = \lambda^{-2}(0)(1 - (T/T_c)^{2.5}) \tag{4}$$

which saturates at low temperatures, like that expected from BCS. This would imply a nodeless energy gap, of s- or p-wave symmetry. In this scenario, the strong suppression of T_c with impurities [9] would however favour p-wave symmetry. Impurities in the sample might also change the temperature dependence of λ from its intrinsic shape. In the HTS, they usually lead to a flattening of $\lambda^{-2}(T)$ versus T at low temperatures.

In conclusion, we have studied the vortex lattice in the novel perovskite superconductor SRO. We find that the field probability distribution is highly consistent with that of a square vortex lattice. We note that this flux lattice structure is also found in samples with higher B_{c_2} and T_c by SANS [10], suggesting that a square vortex lattice is independent of the impurity concentration and is a fundamental property of this system. From the field distribution, together with the observed dependence of B_{c_2}, we also estimate the low-temperature values and temperature dependences of the fundamental superconducting parameters ξ, λ and κ for this sample. The results are similar to those obtained in [4], but a direct comparison is difficult, as the superconducting parameters may be influenced by depairing due to impurities. We can however conclude that SRO has low κ, large ξ and a square flux-line lattice.

Acknowledgments

We would like to thank Chris Baines (PSI) for support with the dilution refrigerator, Ilija Savić for adding colour to the experiment and Alex Shengelaya for providing the sample. Financial support from the EPSRC of the UK and the Swiss National Science Foundation is gratefully acknowledged.

References

[1] Maeno Y, Hashimoto H, Yoshida K, Nishizaki S, Fujita T, Bednorz J G and Lichtenberg F 1994 *Nature* **372** 532
[2] Rice T M and Sigrist M 1995 *J. Phys.: Condens. Matter* **7** L643
[3] Mazin I I and Singh D J 1997 *Phys. Rev. Lett.* **79** 733
[4] Yoshida K, Maeno Y, Nishizaki S and Fujita T 1996 *Physica* C **263** 519
[5] See, e.g.,
Tilley D R and Tilley J 1990 *Superfluidity and Superconductivity* 3rd edn (Bristol: Insitute of Physics Publishing)
[6] Machida K, Ozaki M and Ohmi T 1996 *J. Phys. Soc. Japan* **65** 3720
[7] Rainford B D and Daniell G J 1994 *Hyperfine Interact.* **87** 1129
Aegerter C M, Hofer J, Savić I M, Keller H, Lee S L, Ager C, Lloyd S H and Forgan E M 1998 *Phys. Rev.* B **57** 1253
[8] Sidorenko A D, Smilga V P and Fesenko V I 1990 *Hyperfine Interact.* **63** 49
[9] Mackenzie A P, Haselwimmer R K W, Tyler A W, Lonzarich G G, Mori Y, Nishizaki S and Maeno Y 1998 *Phys. Rev. Lett.* **80** 161
[10] Riseman T M *et al* 1998 *Nature* submitted
[11] Brandt E H 1988 *J. Low Temp. Phys.* **73** 355
[12] Kogan V G, Bullock M, Harmon B, Miranović P, Dobrosavljević-Grujić Lj, Gammel P L and Bishop D J 1997 *Phys. Rev.* B **55** R8693
[13] Eskildsen M R *et al* 1997 *Phys. Rev. Lett.* **78** 1968
Paul D M^{c}K, Tomy C V, Aegerter C M, Cubitt R, Lloyd S H, Forgan E M, Lee S L and Yethiraj M 1998 *Phys. Rev. Lett.* **80** 1517
De Wilde Y, Iavarone M, Welp U, Metlushko V, Koshelev A E, Aranson I and Crabtree G W 1997 *Phys. Rev. Lett.* **78** 4273
[14] Yaouanc A, Dalmas de Réotier P and Brandt E H 1997 *Phys. Rev.* B **55** 11 107
[15] Cubitt R *et al* 1993 *Nature* **365** 407
[16] Tinkham M 1975 *Introduction to Superconductivity* (New York: McGraw-Hill)
[17] See, e.g.,
de Gennes P-G 1965 *Superconductivity of Metals and Alloys* (New York: Addison-Wesley)
[18] Hardy W N, Bonn D A, Morgan D C, Liang R and Zhang K 1993 *Phys. Rev. Lett.* **70** 3999